Exploring temporal aspects of climate-change effects due to bioenergy

Samuel J G Cooper* [a, b], Rowan Green[a, b], Laura Hattam[c], Mirjam Röder[d, e], Andrew Welfle[d, f], Marcelle McManus[a, b]

a Centre for Sustainable and Circular Technologies (CSCT), University of Bath

b Department of Mechanical Engineering, University of Bath

c Institute for Mathematical Innovation (IMI), University of Bath

d Supergen Bioenergy Hub

e Energy and Bioproducts Research Institute (EBRI), Aston University

f Tyndall Centre for Climate Change, University of Manchester

* Corresponding author: sjgcooper@bath.edu, +44 1225 385888, Department of Mechanical Engineering, University of Bath, Bath BA2 7AY, UK

Highlights

- Climate-change effects of two case studies compared to results from carbon-balance
- Single metrics do not always fully convey climate-change impacts
- Spreadsheet tool made available to facilitate assessment of temporal variation in impacts
- Inclusion of additional results recommended to provide complete picture

Abstract

The greenhouse gas emissions associated with bioenergy are often temporally dispersed and can be a mixture of long-term forcers (such as carbon dioxide) and short-term forcers (such as methane). These factors affect the timing and magnitude of climate-change impacts associated with bioenergy in ways that cannot be clearly communicated with a single metric. This is critical as key comparisons that determine incentives and policy for bioenergy are based upon climate-change impacts expressed as carbon dioxide equivalent calculated with GWP100.

This paper explores these issues further and presents a spreadsheet tool to facilitate quick assessment of these temporal effects. The potential effect of (i) a mix of GHGs and (ii) emissions that change with time are illustrated through two case studies. In case study 1, variations in the mix of greenhouse gases mean that apparently similar impacts after 100-years, mask radically different impacts before then. In case study 2, variations in the timing of emissions cause their climate-change impacts (integrated radiative-forcing and temperature change) to differ from the impacts that an emissions-balance would suggest. The effect of taking alternative approaches to considering "CO_2-equivalence" are also assessed.

In both cases, a single metric for climate-change effects was found to be wanting. A simple tool has been produced to help practitioners evaluate whether this is the case for any given system. If complex dynamics are apparent, it is recommended that additional metrics, more detailed inventory, or full time-series impact results are used in order to accurately communicate these climate-change effects.

Keywords

GWP; GTP; dynamic LCA; carbon balance; climate change; bioenergy;

1. Introduction

Bioenergy has been suggested as a key resource of low-carbon, versatile energy vectors. However, the timing and evaluation of its associated emissions (and absorption) of Greenhouse gases (GHGs) has also received significant scrutiny [1–4]. This is appropriate; the recent IPCC special report [5] suggests that we have had a remaining (at the end of 2017) global carbon budget of 420 Gt-CO_2e in order to stay below 1.5°C. Any approaches that we have for optimising systems must fully consider the relevant timescales and take appropriate account of both the short-term impacts as well as the longer timescale traditionally reported within conventional LCA [6,7].

Given the key role that LCA-based carbon accounting is given in policy making and incentives (e.g. RED, RTFO) [8], a full understanding of the temporal effects that may complicate the climate-change impacts of bioenergy is critical. Here, we are concerned with two distinct ways in which metrics expressed as a single figure are unable to appropriately convey climate-change impacts:

1. Otherwise identical emissions that occur at different times will have different effects at a given point in the future. Assuming that all emissions occur at the start of an accounting time horizon ignores this reality.
2. Different mixtures of GHG emissions will result in effects that vary with time differently. Expressing the effects of these mixtures of emissions at a particular point in time gives no indication of how they compare at other points in time.

In this paper, we seek to explore these effects through the use of two case studies. We will start by introducing the mechanisms that lead to these two sensitivities and the metrics that are associated with them. We then go on to discuss various alternative metrics and approaches that have been developed in order to address them. The two bioenergy case studies are then described: (i) Agricultural and forestry wastes to a district heating system, and (ii) Forestry systems used to supply bioenergy for electricity generation. These case studies are taken from other research in which their climate-change impacts are described in terms of carbon dioxide (CO_2) equivalence on the basis of

GWP100. A methods section describes the approach taken to reanalyse these results with different metrics. Novel metrics are introduced to illustrate the fact that possibility that alternative interpretations of "CO_2-equivalence" can present quite different pictures.

2. Background

2.1 Introduction to climate-change metrics and effects

The warming effects of gases is complex and depends upon a range of factors that are hard to incorporate into repeatable metrics that can be readily calculated and understood. Idealised metrics such as Global Warming Potential (GWP) and Global Temperature Potential (GTP) have been developed in order to provide a basis for comparison between them [9,10]. These are based upon simplified models; relating to the change in abundance of the gases after an initial release, a radiative forcing model (typically a constant) and (in the case of GTP) a climate response model.

Figure 1 illustrates the modelled effect of carbon dioxide (CO_2), methane (CH_4) and nitrous oxide (N_2O). Figure 1a shows how the relative abundance of these gases varies with time after an initial pulse emission. These are generally modelled as exponential decays. In the case of CO_2, a slightly more complex model is typically used in order to better capture the response and interaction between different CO_2 sinks such as oceans and plant growth by splitting the decay into several components with different time constants (and one persistent component) [11]. This means that while its abundance decreases rapidly after the initial impulse, the rate of CO_2 decrease reduces towards a (non-zero) long-term equilibrium. This results in more CO_2 than N_2O remaining after around 120 years. In each case it is recognised that the models and parameters will not be constant with time (e.g. as concentrations increase). Parameters for Figure 1 are taken from [9,12].

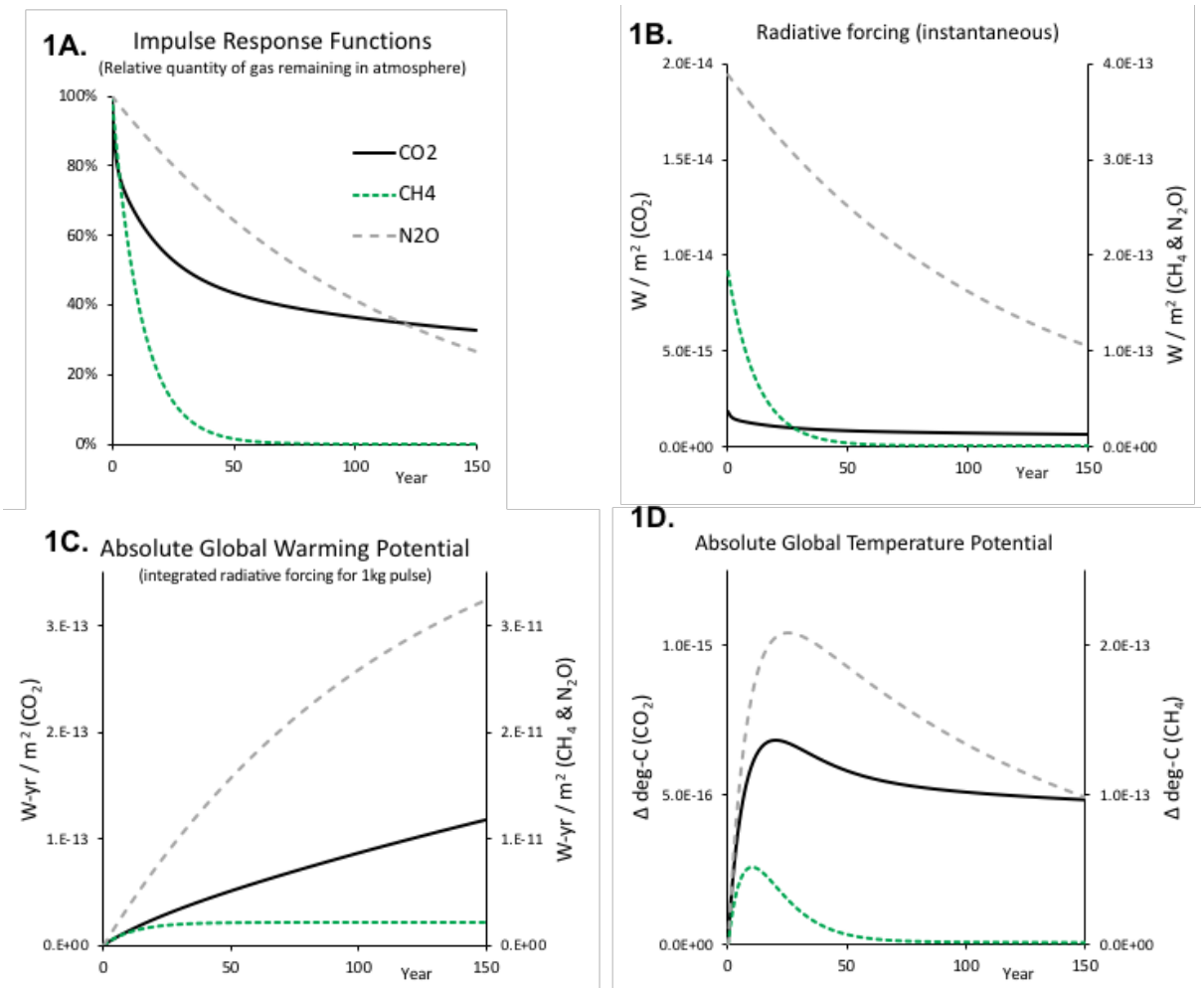

Figure 1: Simplified climate change effects of pulse emissions of CO_2, CH_4 & N_2O. Model parameters taken from [12]

Figure 1b illustrates the evolution of the radiative forcing effect that might be caused (per unit area) by a 1kg impulse emission of these gases. This is based upon the product of the abundance of gas remaining in the atmosphere (i.e. following 1a) and a specific forcing constant defined for each gas. This specific forcing is far greater for N_2O and CH_4 than for CO_2. It is modelled as a constant but in reality depends upon factors (e.g. atmospheric concentration) that relate to the forcing mechanism for that gas, and corresponds to a change at a defined point in the climate system.

Figure 1c shows the time-integral of the radiative forcing (for the same 1kg impulse emissions of gases). That is, the additional net heat (per unit of area) that would have entered the troposphere due to the forcing that occurs up to that point in time, excluding the effects of feedbacks such as surface temperature change. This is the Absolute Global Warming Potential (AGWP) if appropriate

parameters are used. The plots for N_2O and CH_4 are against the right-hand axis (i.e. 100x greater). While the AGWP for CH_4 initially increases rapidly, this rate of increase decreases with the decay of the remaining CH_4 and so is relatively constant (i.e. no increase) after around 40 years. In contrast, while the rate of increase of AGWP for CO_2 initially decreases, the rate becomes almost a linear increase as the CO_2 abundance tends towards its new equilibrium.

Figure 1d illustrates the climatic temperature response to the forcing caused by these emissions. Here, the climate response model relating to Absolute Global Temperature Potential (AGTP) is used. As this model includes a component for re-radiation of heat, it is not purely integrative (in contrast to AGWP). For each emission of gas, there is a peak temperature response followed by a decay. The modelled temperature response to CH_4 is a relatively sharp peak at around 10 years decreasing to almost nothing by 50 years. However, for CO_2 the peak (at around 20 years) is followed by a very gradual reduction before the temperature effect remains almost constant at around 75% of the peak.

A temperature effect is, perhaps, easier to interpret to a physical reality but it should be remembered that warming can result in different damage mechanisms. For each of these, each metric or others might be more or less appropriate as a proxy for relative effect [13,14]. For example, temperature changes might be a proxy for damage relating to heat waves, heating might be a proxy for sea-level or ice melt effects, rate of change (e.g. radiative forcing) might be a proxy for adaptation impacts. For both integrated radiative forcing and temperature effects, it might also be that comparison to a threshold measure, or a time-integration is appropriate [15,16].

GWP and GTP are the AGWP and AGTP results after normalising to the relative effect of an (equal mass) impulse emission of CO_2. As the ratio between the absolute results of different gases changes with time, a GWP or GTP metric is defined relative to a time-horizon.

This results in the two ways in which metrics calculated with a time horizon that is fixed relative to the time of emissions might be unable to appropriately convey warming effects:

1. Otherwise identical emissions that occur at different times will have different effects at a given point in time. Assuming that all emissions occur at the start of an accounting time horizon ignores this reality.
2. Different mixtures of GHG emissions will result in effects that vary with time differently. Expressing the effects of these mixtures of emissions at a particular point in time gives no indication of how they compare at other points in time.

This paper seeks to explore these issues further with the use of two case studies.

2.2 Alternative metrics and approaches

Brandão et al. [14] provide a thorough review of the progression of various methods and approaches towards the first of these sensitivities (the effect of emissions and absorptions occurring at different times). Fifteen approaches are described and can be generally assigned between four groups: i) Approaches that take a static metric such as equivalence based on GWP or GTP; ii) Approaches that apply a ton-year type metric; iii) Approaches that apply a time-horizon for impacts that is independent of the timing of the GHG fluxes (rather than a time-horizon that is relative to them, such as conventionally used in GWP); iv) Approaches that take a combination of impacts (e.g. Kirschbaum's "Climate Change Impact Potential" [13]). Several researchers have developed variations of approach (iii), focussing on different sources of emissions and boundaries, notably [17–21]. Cherubini et al's presentation of this paradigm as the convenient GWP_{bio} metric [20] has subsequently been extended by others (e.g. [21]).

Various approaches have also been suggested to communicate the effect of a combination of GHGs [7,22–24]. In some cases, there are implicit value-judgements in achieving this, that might or might not align with the way in which the metrics are then used. In this regards, the limitations of GWP100 as a metric are accepted, even as its broad use is recognised [15]. Papers [22–24] extensively report on workshops to determine best practice for LCA and appropriate approach to the issue of climate-change metrics. A step-by-step approach is recommended, in which sensitivities are explored and

then additional metrics (e.g. based on GTP100 or GWP20) used as appropriate to communicate these.

In some cases, full time-dependent plots of climate-change impacts are provided as examples (e.g. [16,25–28]). These studies typically provide excellent sensitivity analysis and a far-fuller picture of the results. However, they are unfortunately quite rare.

This paper therefore aims to build upon previous literature with several additional contributions:

- Data relating to additional case studies that further illustrate the effect of including a temporal scope.
- Illustration of the effect of reanalysing existing case studies with this approach. Considering both the timing of emissions and their characteristics, with both integrated radiative forcing and instantaneous temperature impacts.
- Provision of a spreadsheet to facilitate other researchers and practitioners in considering this sensitivity.
- Introduction of additional metrics in assessing the contribution of GHG fluxes that have occurred up to a point in time, as part of an impact at a future point in time.

3. Description of case studies

Two case studies have been selected from the literature and reanalysed to illustrate the way in which temporal effects can be masked by single-metric results. They have been selected to provide examples of the potential effect of (i) A mix of GHGs, and (ii) Emissions occurring over a period of time. While the case-studies are based on bioenergy systems, it should be apparent that many other systems may share one of these conditions.

3.1 Case study 1: District heating networks supplied by bioenergy

This case study is taken from analysis by Green [29]. The climate-change effects of a wide range of bioenergy options to supply heat to a district heating network (DHN) were compared. In total, over 300 options were studied. Her study investigated several bioenergy feedstocks: forest residue pellets, forest residue woodchips, stemwood chips, stemwood pellets and wet manure. Heat provision options of CHP to DHN, boiler to DHN, and gas grid injection were compared. Other variations considered different national background data, different biomass transport distances (up to 500km) and different counterfactual fuels (coal, peat, natural gas).

The primary GHG assessment was performed in BioGrace-II [30] in order to be compatible with relevant reporting standards and facilitate repeatability. Full methods are provided in Green, with supplementary information providing details of parameters and assumptions (also see Supplementary Information to this paper). Results from the study are illustrated in Figure 2. Here, avoided emissions due to counterfactual heat provision are not included. Figure 2 contrasts the climate-change effect due to CO_2, to that due to CH_4 and N_2O (using GWP100 for equivalence). On the left, this is illustrated as total GHG emissions against the proportion relating to CO_2. On the right, this is illustrated as CO_2 emissions against CH_4 and N_2O emissions.

Four examples (highlighted as green circles) were selected for further study. These cover different (but not outlying) total global warming effects, with a mix of contributions from different GHGs. In

two of the examples that relate to anaerobic digestion (AD), the effect of avoided CH_4 emissions (due to alternative treatment of slurry) is roughly equivalent to the effect of CO_2 emissions (if using GWP100 for equivalence). In the other two examples, relating to use of forest residues, the main GHG flux is CO_2 emissions. The overall warming results for these four examples are given in Table 1. In each case, all relevant GHG fluxes (emissions, biogenic absorption and avoided emissions) are assumed to occur as a single event in year-0.

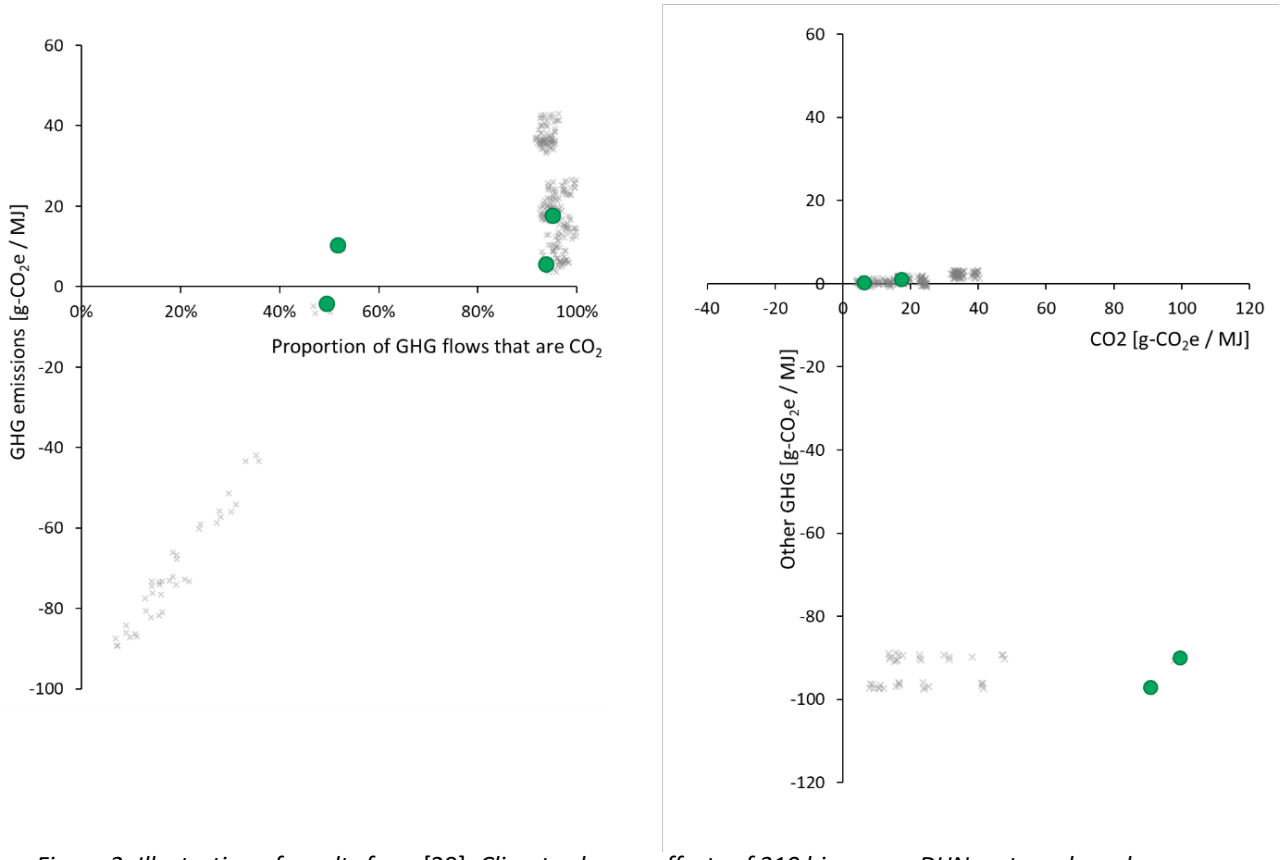

Figure 2: Illustration of results from [29]*. Climate change effects of 310 bioenergy DHN systems based on BioGrace-II with CO_2 equivalence based on GWP100. Examples for further analysis highlighted as green circles.*

Table 1: CO_2 equivalence based on GWP100 for examples selected from [29] *(highlighted as circles in Figure 2)*

System	g- CO_2e/MJ (GWP100)
1. Biogas to CHP	-4.0
2. Biomethane injection	9.8
3. Forest residue chips	6.0
4. Forest residue pellets	19.0

3.2 Case study 2: Forestry lifecycle

This case study is taken from analysis by Röder et al. [31]. In their study, the time-dependent emissions of GHGs from six scenarios are modelled. These relate to bioenergy from three different forest systems (US, Spain, Canada), with two variations each, being supplied to generate electricity in the UK. In the US and Canadian forest scenarios, the forest systems primarily produce wood products (with 25-year and 70-year rotations respectively) and the bioenergy is derived from harvest residues, sawmill residues and thinnings. In the Spanish forest scenario, Eucalyptus is grown exclusively for bioenergy with a 32-year rotation (with coppicing after 16 years). Emissions due to forest activities, processing and transporting the bioenergy are comprehensively evaluated while the net carbon balance of the forest systems (including soil) is modelled in CO2FIX. Net and cumulative emissions are calculated at the levels of both forest stand and whole forest (i.e. at sufficient forest size that the total biomass extractions balance growth). Figures 3 and 4 are adapted from their results to illustrate them. For each of the forest systems, only one of the two scenarios (variant “a”) is used as an example here. The results for the forest stands (Figure 3) are aligned with a harvest in year-0 (i.e. with the baseline for zero emissions set just before this harvest). For the whole forest (Figure 4), there is a harvest each year, rotating across the different stands (with activities such as thinnings in other stands as appropriate). The figures presented here are attributional results that do not consider CO_2 that would have still been absorbed by the mature forests if not managed, nor include any fossil-fuel emissions avoided by the use of bioenergy (although these are assessed in the original study).

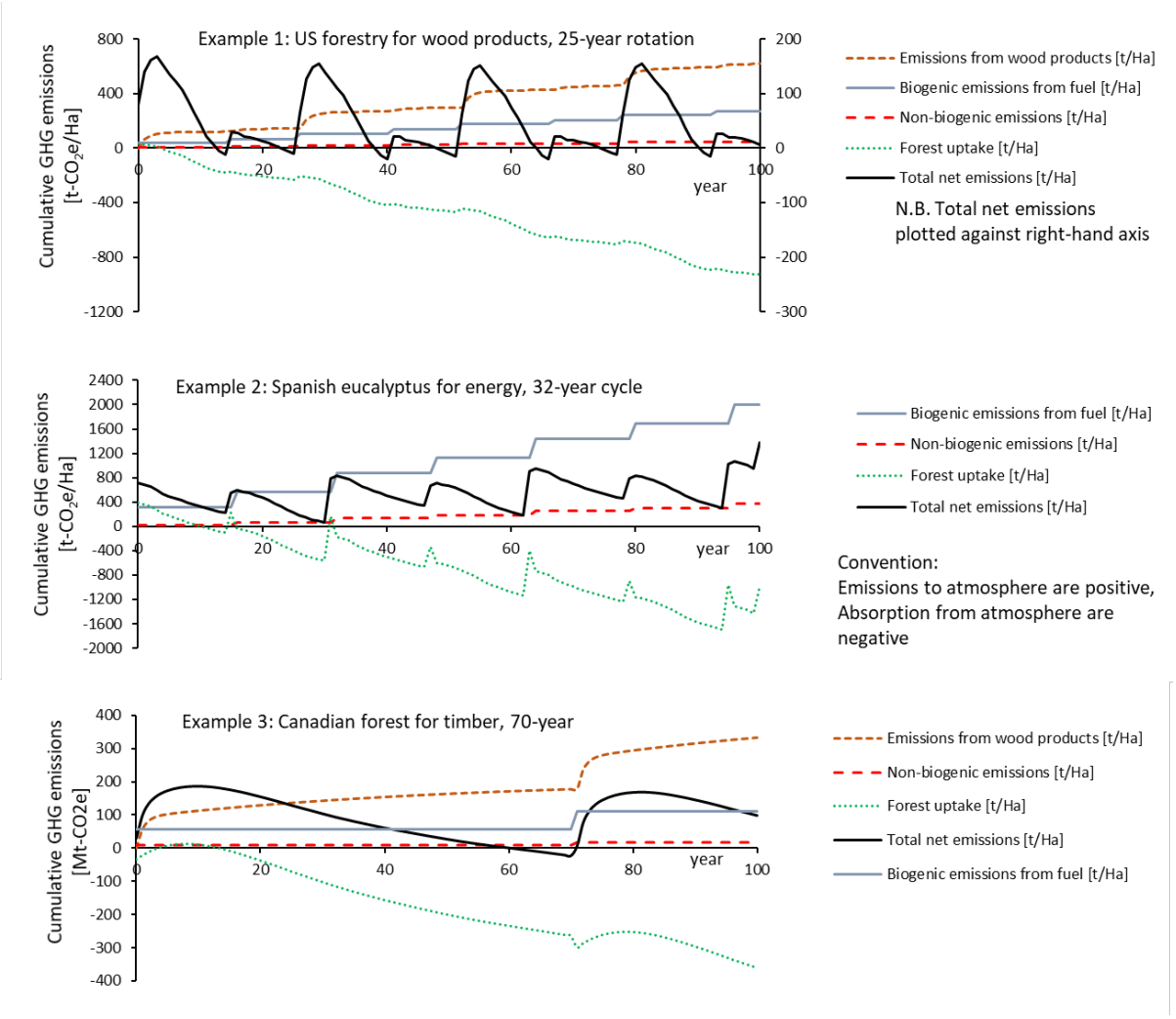

Figure 3: Cumulative GHG emissions at forest-stand level. CO_2 equivalence based on GWP-100. Note that the total net emissions for example 1 are plotted against the right-hand axis. Adapted from [31]

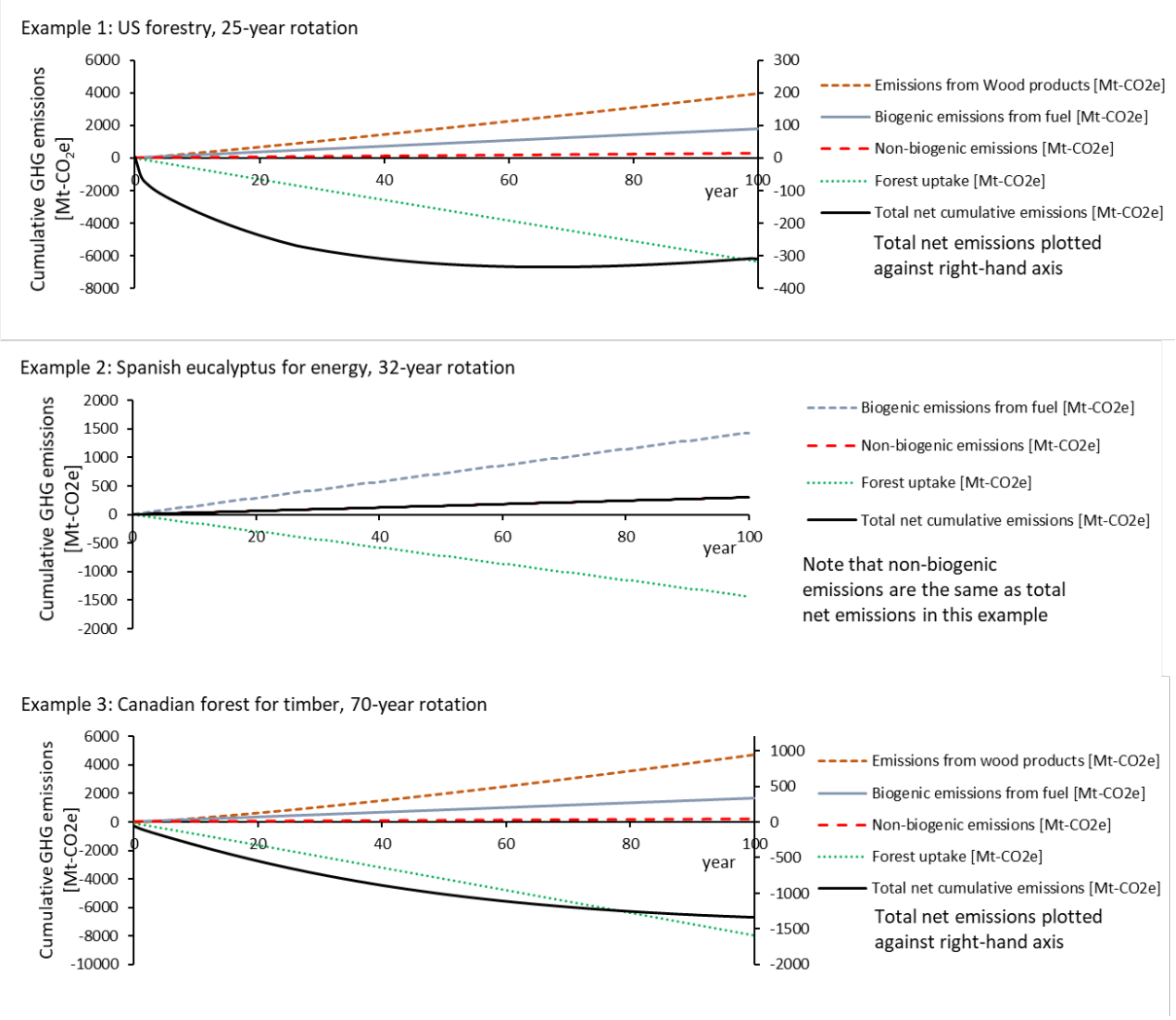

Figure 4: Cumulative GHG emissions at whole forest level. Note that the total net emissions for examples 1 and 3 are plotted against the right-hand axis. Adapted from [31]

At the level of an individual stand there is significant year-on-year variation, but this is smoothed out across the whole forest as the stands are harvested in rotation. Over most years and cumulatively, the forest absorbs CO_2 as expected, albeit with slight net emissions from stands that have just been harvested. The CO_2 sequestered in wood products from a forest stand is greatest just after a harvest, before decreasing as products reach the end of their life and are combusted (this rate is assumed to be a function of their stock). Across the forest, the emissions from wood products reaching their end of life increases at a slightly increasing rate in line with their increasing stocks. Cumulative biogenic emissions from burning pellets and non-biogenic emissions from other activities increases in steps at the stand level, corresponding to the years in which harvest or other activities take place. Across the whole forest, this results in linear trends for both of these emissions sources. The net results of

these fluxes is often relatively small compared to the overall CO_2 absorbed by the forest and then re-emitted from pellets and wood products (as such, it is plotted on secondary axis for several graphs in Figures 3 and 4). At whole-forest level, it is negative in the examples in which wood products are produced (#1 and #3) but positive (equivalent to non-biogenic emissions) in the example where forestry is used only for bioenergy (#2). At a stand level, the net cumulative emissions follow a similar trend on average but are positive for most of the time due to the starting point in the lifecycles (harvesting) that has been selected.

4. Methods

Standard equations (in studies [12,32] corresponding to AGWP, and study [10] corresponding to AGTP, using parameters from [12,32,33]) were used to assess the integrated radiative forcing and instantaneous temperature effects due to each of the case study examples. This was performed on a year-by-year basis; i.e. the integrated radiative forcing and temperature change effects occurring each year due to each prior emission (or absorption) of CO_2, CH_4 and N_2O were calculated.

Practically, this method was implemented in an excel spreadsheet in which the net emissions (or absorption) of each gas are entered as a year-by-year inventory. Here, a recursive approach was developed in which the results for a given year are calculated on the basis of that year's inventory and the results of the previous year. This is in contrast to previous approaches in which a full time-series of results from each year's inventory items was calculated and then these results were added together. The recursive approach greatly simplifies the spreadsheet relative to the alternative approach of calculating the full time-dependent results of each year's emissions separately and then summing them together. It enables calculations of the full time-dependent climate effects to be performed rapidly (in O(n) time rather than $O(n^2)$ time) and easily whilst maintaining the transparency and accessibility of a spreadsheet. The details of this approach are expanded in Appendix 1 to assist other researchers develop similar models; it will improve relative performance even further if some future application calls for results calculated with shorter time-steps. The spreadsheet is available as Supplementary Information to this paper and as [34] for other researchers to use or adapt.

Because this approach takes account of the timing of the emission and absorption of gases when summing their effects, the resulting integrated radiative forcing and instantaneous temperature change effects at a particular point in time are different to those that would be calculated with a conventional (sliding time horizon) approach (where the timing of emissions does not affect their

reported effects). Rather, these results are equivalent to those determined with a time horizon for impacts that is independent of the timing of GHG fluxes (i.e. as per e.g. [17,18,21]).

These results were normalised to the effect of a CO_2 pulse at year-0; expressing them in terms of CO_2-equivalent mass. This was also done on a year-by-year basis, i.e. for the temperature change occurring due to the system *each year*, the mass of CO_2 emitted in year-0 that would result in an equivalent temperature change *in that year*.

When assessing the effect of emissions occurring up to a certain time, it might be relevant to express this in terms of the equivalent year-0 CO_2 emission that would cause the same effect up to that point, but it might also be relevant to express the impact in terms of the equivalent year-0 CO_2 emission that will cause the same effect at a future time of interest (e.g. for policy purposes, reporting on the amount of a "carbon budget" that has been spent, or the future impact that will have been "committed to" by a certain point). For the forest systems (Case study 2), additional (and to our knowledge, novel) integrated radiative forcing and instantaneous temperature metrics were developed and used with this consideration. These are the "CO_2 equivalent in terms of contribution to integrated radiative forcing by [or temperature at] year-100". By this it is meant, for each year, the mass of CO_2 emitted in year-0 that would result in an equivalent integrated radiative forcing [temperature change] effect by [at] year-100, as the cumulative emissions up to that year would result in by year-100 (i.e. if no other emissions occur after that point).

These metrics can be thought of as equivalent to the contribution of emissions up to that point to the final integrated radiative forcing [or temperature change] effect at year-100. Or alternatively, when the emissions causing the final effect actually occur. In a sense, they are examples of "forward looking" metrics, in that they illustrate the effect that emissions up to a certain time will have at a point in the future. This is in contrast to metrics that consider effects that occur up to that point (or at) that point in time.

4.1 Limitations to analysis

It is important that Life Cycle Assessment (LCA) studies fully report upon their limitations [35]. The analysis presented here is not a full LCA but still contains several sources of uncertainty. Relevant to the Impact Assessment and Interpretation steps that we are focussing on, are significant uncertainties around the radiative forcing and temperature response of different species. Clearly, there are additional uncertainties and simplifications in the climate response to forcing that is assumed when assessing temperature responses.

Other effects can cause significant climate change effects but have not been included. The aim of this study is to demonstrate the significance of temporal aspects to climate change impacts and provide a tool to facilitate the assessment of some of them. However, it is not comprehensive in its coverage of mechanisms that can affect the climate. These mechanisms include bio-geophysical effects due to changes in surface albedo, evapotranspiration and surface roughness. These factors have significant climate effects in addition to those relating directly to radiative forcing. In the spreadsheet tool prepared as part of this study, provision is made for users to manually add radiative forcing elements that do not relate to emissions but this is not fully expanded to include a model of any underlying mechanism – it is primarily intended to enable quick comparison of how their temporal effect might compare to the system under consideration.

Several near-term climate forcers are absent from the analysis presented here and from the spreadsheet model. In particular these relate to species that have large indirect effects and are better approached with multi-component models [36]. These species often have effects that are dependent on location (latitude and / or altitude) and timing (e.g. season of year).

Again, it is noted that the purpose of this analysis is to demonstrate the relative magnitude of temporal effects but it should be noted that these additional effects are worthy of additional attention.

5. Results and discussion

5.1 Case study 1: DHN with bioenergy examples

The four examples in this case study illustrate the effect of combining emissions of different gases that occur at the same time but have different characteristics. For the four district-heating network (DHN) examples, Figure 5 illustrates the time-dependence of the integrated radiative forcing and instantaneous temperature effects. That is, the evolution with time of these effects due to a pulse release / absorption of different quantities of CO_2, CH_4 and N_2O in year-0 (as per the original results for the examples). The overall effects that are plotted are the result of combining the different dynamic effects from each of these releases or absorptions.

In Figure 6, these results are expressed in terms the mass of CO_2 released in year-0 that would have an equivalent effect for each year.

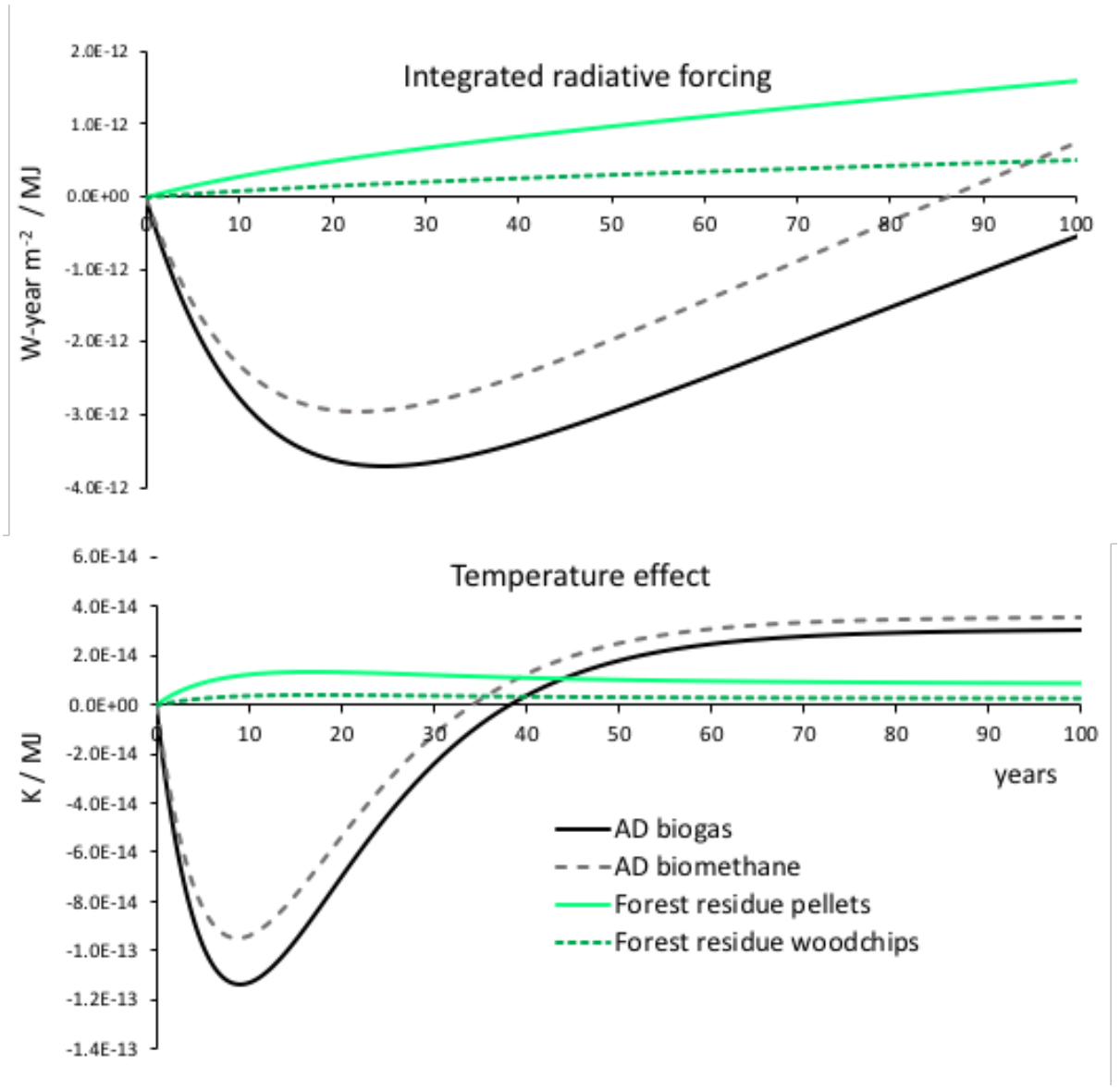

Figure 5: Variation with time of integrated radiative forcing and temperature effects that would occur due to DHN examples.

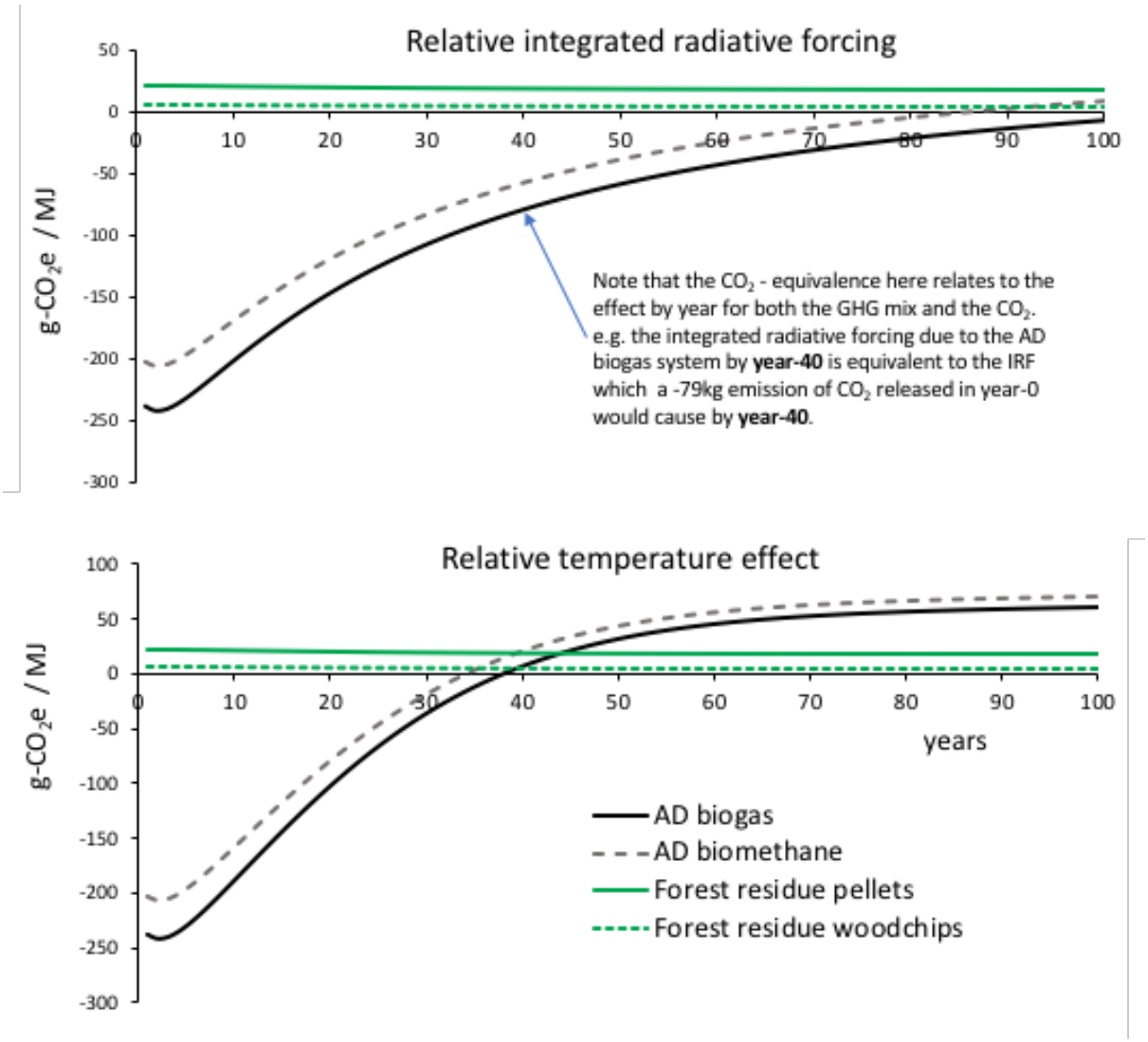

Figure 6: Variation with time of integrated radiative forcing and temperature effects expressed as CO_2-equivalent.

Emissions in the two forest residue examples are dominated by CO_2. As a result, these results are relatively straightforward, with integrated radiative forcing increasing steadily as time from the initial emission increases, and temperature change remaining fairly consistent. The CO_2 equivalent masses for these two examples are constant with respect to time.

Emissions in the two Anaerobic Digestion (AD) examples are more complicated; in the original results, more CO_2 is emitted but some CH_4 emissions are avoided due to the treatment of slurry. This results in far more complex climate effects. For example, 100 years after the emissions, the integrated radiative forcing resulting from each example is similar to the forest residue options (-

$6x10^{-13}$ to $+16x10^{-13}$ W-year/m^2, CO_2-equivalents given in Table 1) but this obscures the fact that the AD examples result in net cooling (negative integrated radiative forcing) that is far more pronounced for most of the intervening period.

The temperature effects for the two AD examples are even less intuitive from the final (100 year) results. At this point (after 100 years) they result in significantly greater temperature increases than the forest residue options. However, for the first 34 to 38 years, they result in a temperature ***decrease*** that is most pronounced around 10 years after the initial emission. Comparing the two metrics, it is notable that not only do the relative magnitudes of each metric vary with time, but that their signs also change at different times. Fifty years after the initial emissions, the AD examples have caused a negative integrated radiative forcing (i.e. cooling) effect at the same time as a temperature increase.

5.2 Case study 2 – Forest lifecycle examples

The three forest examples in this case study illustrate the effect of combining emissions that are mainly CO_2 but that occur at different times. The variation in these effects is the result of the combination of the temporal emissions profiles and the dynamics of the effects that are due to them. Figure 7 illustrates the effects of ongoing GHG emissions at the forest-stand level for the three forest examples. Figure 8 illustrates these effects at whole-forest level. In each case, the "Cumulative GHG net emissions" plots are exactly the same as the "total net cumulative emissions" plots from Figures 3 and 4.

The plots for each metric are discussed below but it is firstly instructive to note the significant difference between what might otherwise be assumed to be similar metrics (with the same units, here Mt-CO_2e or t-CO_2e/Ha) and their variation with time. Clearly, an understanding of what they actually mean and the implications of differences between them is important.

In each case, the actual change in atmospheric GHG at any given point due to the forestry is not the same as the total net cumulative emissions up to that point; its magnitude progressively reduces

relative to the cumulative emissions due to the effect of sinks outside of the system (e.g. oceans) and the decay of the GHG gases. Although this difference occurs across each example at both forest-stand and whole-forest levels, the ratio between them is dependent upon each temporal emissions profile and cannot be accurately predicted without this. While Figure 7 demonstrates the complexity of the relationship between the different effects of these temporal GHG fluxes, they are easier to interpret from the simpler averaged dynamics in Figure 8 and so these are discussed below. However, the underlying causes are the same for both cases.

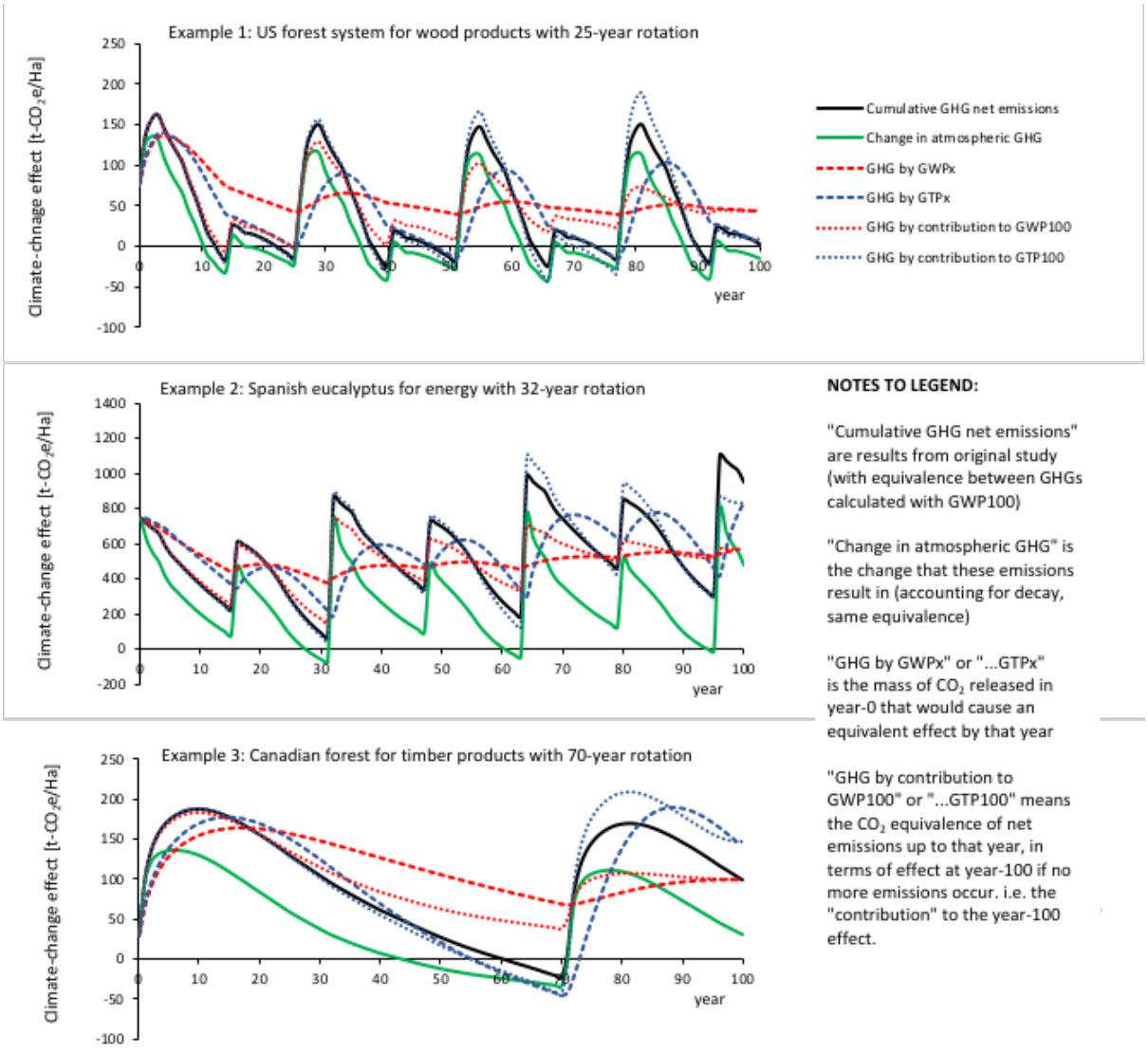

Figure 7: Temporal effects of ongoing GHG emissions due to forest-stand activity

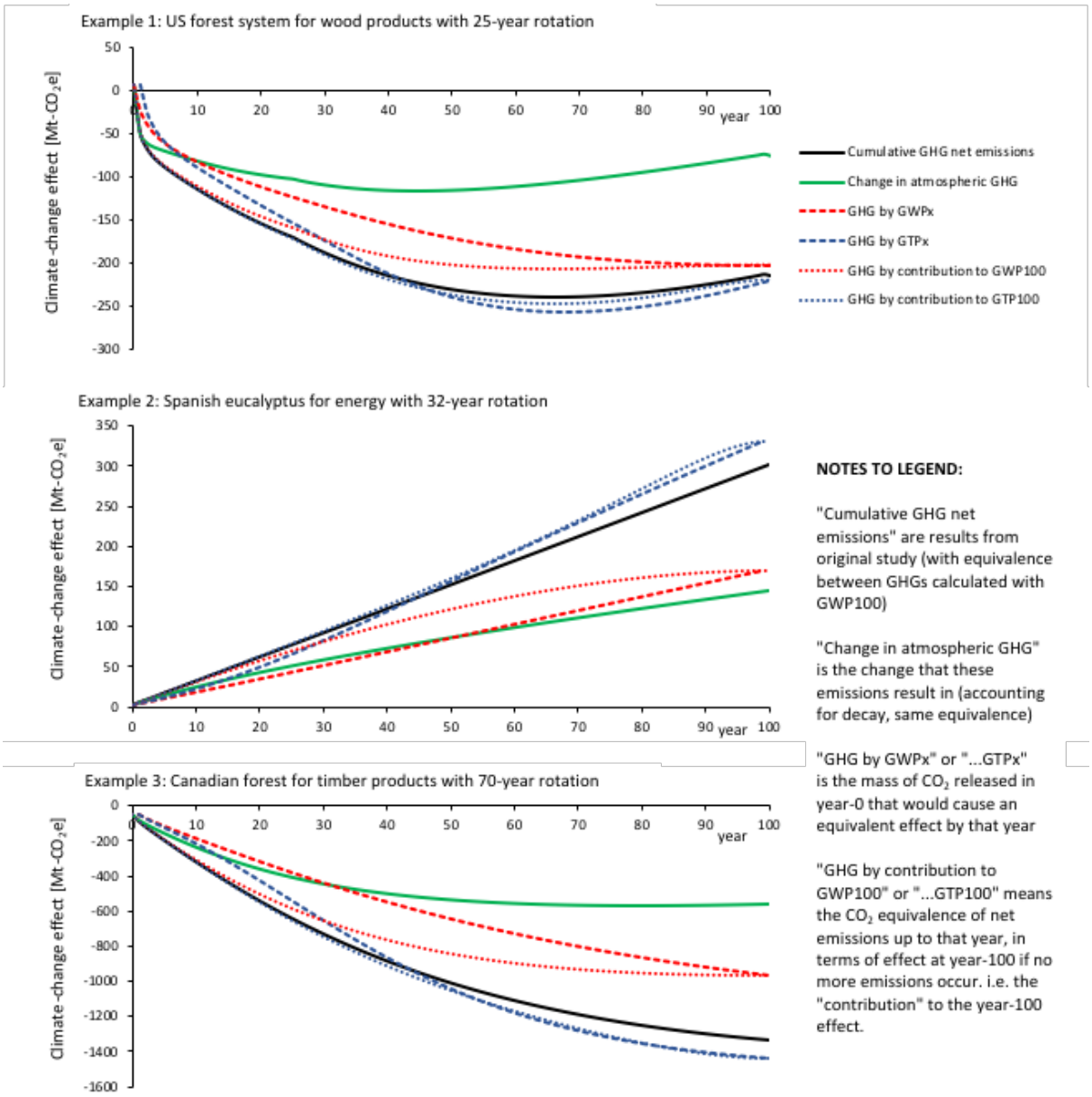

Figure 8: Temporal effects of ongoing GHG emissions due to whole-forest activity

Here (Figures 7 and 8), the "GHG [equivalent] by GWPx" and "… GTPx" plots refer to the quantity of CO_2 released at year-0 that would cause an equivalent integrated radiative forcing or temperature change effect (respectively) by that year. For example, at year-50 on the x-axis, the GHG by GWPx plot refers to the mass of CO_2 that would cause equivalent integrated radiative forcing by year-50 if released at year-0. At year-100 on the x-axis, these plots provide the values that would be derived from a 100-year time horizon that is independent from timing of emissions (i.e. equivalent to Levasseur's dynamic approach or similar, e.g. [17,18,21]) but they also provide the progression up to

that point. These are typically different from the total net cumulative GHG emissions figures that might conventionally be used to compare climate change impacts and concepts such as “carbon neutrality”.

The ongoing nature of GHG fluxes within the whole-forest systems means that the integrated radiative forcing effect (measured as “GHG [equivalent] by GWPx”) is typically less than the cumulative net emissions as some of the emissions won’t have had as much time to contribute to heating. Conversely, while the instantaneous temperature effect (“… GTPx”) metric is generally similar to the cumulative net emissions, it tends to start less (as the atmosphere takes time to warm) and then becomes greater than the cumulative net emissions as the final temperature effects are temporally closer to the actual emissions causing them than the hypothetical pulse at year-0 that their equivalence is expressed relative to.

Despite the fluctuating nature of cumulative net emissions at the forest-stand level (Figure 7), the integrative nature of GWP means that this metric varies less. The temperature effect also varies less when the forest rotations are sufficiently short that the integrative element of the temperature increase can smooth the effect of the emissions fluctuations (e.g. notably in example 2 at forest-stand level).

The plots showing effects expressed as “GHG [equivalent] by contribution to GWP100” and “…GTP100” are the integrated radiative forcing and instantaneous temperature effects that would result at year-100 due to the net cumulative emissions up to that point in the plot. For example, the “GHG [equivalent] by contribution to GWP100” at year-10 is the integrated radiative forcing that would result by year-100 if all emissions fluxes stopped at year-10, expressed in terms of the mass of CO_2 that would cause the same effect by year-100 if released at year-0. This novel metrics show the significance of cumulative emissions up to that year in causing the effects at the year-100 time point. At year-100, these plots converge on the “GHG by GWPx” and “…GTPx” plots (respectively) as they also give results equivalent to those with an independent time horizon.

For integrated radiative forcing effects, these plots ("GHG by contribution to GWP100") show a greater proportional contribution from earlier emissions (starting as equivalent to actual cumulative net emissions) as their heating effect is integrated over the longer time period before year-100.

For temperature effects, these plots ("GHG by contribution to GTP100") are similar to those for cumulative net emissions in early years as the long-term temperature effect of a pulse emission of CO_2 is relatively consistent. However, in later years (i.e. the 20 years approaching the year-100 point), they often have values that exceed the cumulative net emissions as short-term temperature effects become relevant, before they then converge with the "GHG by GTP100" plots by year-100.

For many applications, calculating "CO_2-equivalence" based on CO_2 emissions in year-0 that would have the same effect by the point in time of interest, is a sensible improvement on conventional "sliding time horizon" approaches [17,18,21]. For other applications, it is possible that it is more intuitive to consider the "equivalence" of emissions up to a point, based on the CO_2 emissions in year-0 that would "commit" to the same impact at some specific point in the future. Of concern here is the observation that while the distinction between these approaches seems subtle, the results can be significantly different – for this case study, the main difference occurs at around year-50 for the integrated radiative forcing based equivalencies but this result is specific to the dynamics of the system being assessed (e.g. compare to Figure 7). Again, there is a tension between expressing a full set of results and deriving relevant metrics that can be easily shared. There is not a simple solution to this but having easy access to see the full time-series of results can at least help researchers to make informed choices about presentation of results.

6. Conclusions and Recommendations

The effect of using a range of climate effect metrics with different time boundaries has been studied for two case studies. It is clear that a single figure based on GWP100 is inadequate to convey the full range of these metrics and may not reflect results in the way that decision-makers interpret it to.

Adoption of additional metric to GWP100 (as per recommendations in [7,22–24]) certainly helps and is an encouraging development. However, even there, the full range of results and their appropriate interpretation is hard to fully convey for some systems. The combined effects of long-life and short-life climate forcers can mask the dynamics of what is actually occurring.

We recommend that LCA practitioners and others assessing results relating to climate-change assess the full time-dependent effects of the emissions that they are assessing. They can then make an informed decision about whether using one or two metrics to convey this is adequate or whether more explicit communication of their results is warranted. This could take the form of time-dependency plots or ensuring that GHG emissions are disaggregated by time and by gas in the relevant inventories to ensure interpretation against other criteria is possible in the future (as recommended, for example, by [14,23]). In both cases, this could be supplemented with qualitative notes regarding any significant variations in effects from those that might be anticipated from single figure metrics (e.g. noting the wide range of effects illustrated in Figure 5).

We have made a spreadsheet tool available to facilitate this and remove barriers to practitioners assessing the time dependency of their climate-change results (see Supplementary information or [34]). The equations and analysis are well known and used within the community, but this format may increase their accessibility. It is hoped that enabling rapid and easy assessment of these effects will encourage their consideration.

GHG emissions that occur over a period of time (e.g. net CO_2 from a forest stand) will result in lower integrated radiative forcing than the same GHGs emitted as a pulse in year-0 (as noted by several

researchers and discussed in Section 2, above). In contrast, the temperature effect of CO_2 emissions is far less dependent upon their timing (especially beyond the first 20 years after their emission). However, climate change presents many potential sources of damage. These damage mechanisms will relate in different ways to climate change effects and are not fully understood [13,14]. For example, there may be significant impacts that align more with overall heat input (e.g. ice melting) or rate of temperature increase (e.g. adaptation) than with absolute temperature increase. There is also the possibility of positive-feedback loops (e.g. permafrost melting and releasing more methane) or some damage mechanisms having particular thresholds. Therefore, while there may be some merit in the suggestion of focussing on longer-life climate forcers over short-life climate forcers (as these will tend to relate more closely to future temperature increase [23]), this should not be exclusive. There are complex interactions and a holistic picture is to be preferred.

Acknowledgements

Funding: This research was supported by the Supergen Bioenergy Hub, funded by UKRI grant EP/S000771/1

We are grateful for the valuable suggestions and comments made by two anonymous reviewers.

References

[1] P. Thornley, P. Gilbert, S. Shackley, J. Hammond, Maximizing the greenhouse gas reductions from biomass: The role of life cycle assessment, Biomass and Bioenergy. 81 (2015) 35–43. https://doi.org/10.1016/j.biombioe.2015.05.002.

[2] M. Röder, C. Whittaker, P. Thornley, How certain are greenhouse gas reductions from bioenergy? Life cycle assessment and uncertainty analysis of wood pellet-to-electricity supply chains from forest residues, Biomass and Bioenergy. 79 (2015) 50–63. https://doi.org/10.1016/j.biombioe.2015.03.030.

[3] H. Haberl, D. Sprinz, M. Bonazountas, P. Cocco, Y. Desaubies, M. Henze, O. Hertel, R.K. Johnson, U. Kastrup, P. Laconte, E. Lange, P. Novak, J. Paavola, A. Reenberg, S. van den Hove, T. Vermeire, P. Wadhams, T. Searchinger, Correcting a fundamental error in greenhouse gas accounting related to bioenergy, Energy Policy. 45 (2012) 18–23. https://doi.org/10.1016/j.enpol.2012.02.051.

[4] T.D. Searchinger, T. Beringer, B. Holtsmark, D.M. Kammen, E.F. Lambin, W. Lucht, P. Raven, J.P. van Ypersele, Europe's renewable energy directive poised to harm global forests, Nat. Commun. 9 (2018) 10–13. https://doi.org/10.1038/s41467-018-06175-4.

[5] IPCC, Global Warming of 1.5°C. An IPCC Special Report on the impacts of global warming of 1.5°C above pre-industrial levels and related global greenhouse gas emission pathways, in the context of strengthening the global response to the threat of climate change, International Panel on Climate Change, 2018.

[6] J. Rogelj, D. Huppmann, V. Krey, K. Riahi, L. Clarke, M. Gidden, Z. Nicholls, M. Meinshausen, A new scenario logic for the Paris Agreement long-term temperature goal, Nature. 573 (2019) 357–363. https://doi.org/10.1038/s41586-019-1541-4.

[7] I.B. Ocko, S.P. Hamburg, D.J. Jacob, D.W. Keith, N.O. Keohane, M. Oppenheimer, J.D. Roy-

Mayhew, D.P. Schrag, S.W. Pacala, Unmask temporal trade-offs in climate policy debates, Science (80-.). 356 (2017) 492–493. https://doi.org/10.1126/science.aaj2350.

[8] C. Whittaker, M.C. McManus, G.P. Hammond, Greenhouse gas reporting for biofuels: A comparison between the RED, RTFO and PAS2050 methodologies, Energy Policy. 39 (2011) 5950–5960. https://doi.org/10.1016/j.enpol.2011.06.054.

[9] G. Myhre, F. D. Shindell, .-M. Bréon, W. Collins, J. Fuglestvedt, J. Huang, D. Koch, J.-F. Lamarque, D. Lee, B. Mendoza, T. Nakajima, A. Robock, G. Stephens, T. Takemura, H. Zhang, Anthropogenic and Natural Radiative Forcing, in: T.F. Stocker, D. Qin, G.-K. Plattner, M. Tignor, S.K. Allen, J. Boschung, A. Nauels, Y. Xia, V. Bex, P.M. Midgley (Eds.), Clim. Chang. 2013 Phys. Sci. Basis. Contrib. Work. Gr. I to Fifth Assess. Rep. Intergov. Panel Clim. Chang., Cambridge University Press, Cambridge, n.d.: pp. 659–740. https://doi.org/10.1017/CBO9781107415324.018.

[10] K.P. Shine, J.S. Fuglestvedt, K. Hailemariam, N. Stuber, Alternatives to the global warming potential for comparing climate impacts of emissions of greenhouse gases, Clim. Chang. 68 (2005) 281–302.

[11] F. Joos, R. Roth, J.S. Fuglestvedt, G.P. Peters, I.G. Enting, W. Von Bloh, V. Brovkin, E.J. Burke, M. Eby, N.R. Edwards, T. Friedrich, T.L. Frölicher, P.R. Halloran, P.B. Holden, C. Jones, T. Kleinen, F.T. Mackenzie, K. Matsumoto, M. Meinshausen, G.K. Plattner, A. Reisinger, J. Segschneider, G. Shaffer, M. Steinacher, K. Strassmann, K. Tanaka, A. Timmermann, A.J. Weaver, Carbon dioxide and climate impulse response functions for the computation of greenhouse gas metrics: A multi-model analysis, Atmos. Chem. Phys. 13 (2013) 2793–2825. https://doi.org/10.5194/acp-13-2793-2013.

[12] J.S. Fuglestvedt, K.P. Shine, T. Berntsen, J. Cook, D.S. Lee, A. Stenke, R.B. Skeie, G.J.M. Velders, I.A. Waitz, Transport impacts on atmosphere and climate: Metrics, Atmos. Environ.

44 (2010) 4648–4677. https://doi.org/10.1016/j.atmosenv.2009.04.044.

[13] M.U.F. Kirschbaum, Climate-change impact potentials as an alternative to global warming potentials, Environ. Res. Lett. 9 (2014). https://doi.org/10.1088/1748-9326/9/3/034014.

[14] M. Brandão, M.U.F. Kirschbaum, A.L. Cowie, S.V. Hjuler, Quantifying the climate change effects of bioenergy systems: comparison of 15 impact assessment methods, GCB Bioenergy. (2018). https://doi.org/10.1111/gcbb.12593.

[15] G. Plattner, T. Stocker, P. Midgley, M. Tignor, IPCC Expert Meeting on the Science of Alternative Metrics Edited by IPCC Expert Meeting on the Science of Alternative Metrics, 2009. https://www.ipcc.ch/site/assets/uploads/2018/05/expert-meeting-metrics-oslo.pdf r.

[16] J. Giuntoli, A. Agostini, S. Caserini, E. Lugato, D. Baxter, L. Marelli, Biomass and Bioenergy Climate change impacts of power generation from residual biomass, Biomass and Bioenergy. 89 (2016) 146–158. https://doi.org/10.1016/j.biombioe.2016.02.024.

[17] M. O'Hare, R.J. Plevin, J.I. Martin, A.D. Jones, A. Kendall, E. Hopson, Proper accounting for time increases crop-based biofuels' greenhouse gas deficit versus petroleum, Environ. Res. Lett. 4 (2009). https://doi.org/10.1088/1748-9326/4/2/024001.

[18] A. Levasseur, P. Lesage, M. Margni, L. Deschênes, R. Samson, Considering Time in LCA: Dynamic LCA and Its Application to Global Warming Impact Assessments, Environ. Sci. Technol. 44 (2010) 3169–3174. https://doi.org/10.1021/es9030003.

[19] A. Kendall, Time-adjusted global warming potentials for LCA and carbon footprints, Int. J. Life Cycle Assess. 17 (2012) 1042–1049. https://doi.org/10.1007/s11367-012-0436-5.

[20] F. Cherubini, A.H. Strømman, E. Hertwich, Effects of boreal forest management practices on the climate impact of CO2 emissions from bioenergy, Ecol. Modell. 223 (2011) 59–66. https://doi.org/10.1016/j.ecolmodel.2011.06.021.

[21] G. Guest, F. Cherubini, A.H. Strømman, Global Warming Potential of Carbon Dioxide Emissions from Biomass Stored in the Anthroposphere and Used for Bioenergy at End of Life, 17 (2012). https://doi.org/10.1111/j.1530-9290.2012.00507.x.

[22] A. Levasseur, O. Cavalett, J.S. Fuglestvedt, T. Gasser, D.J.A. Johansson, S. V. Jørgensen, M. Raugei, A. Reisinger, G. Schivley, A. Strømman, K. Tanaka, F. Cherubini, Enhancing life cycle impact assessment from climate science: Review of recent findings and recommendations for application to LCA, Ecol. Indic. 71 (2016) 163–174. https://doi.org/10.1016/j.ecolind.2016.06.049.

[23] F. Cherubini, J. Fuglestvedt, T. Gasser, A. Reisinger, O. Cavalett, M.A.J. Huijbregts, D.J.A. Johansson, S. V. Jørgensen, M. Raugei, G. Schivley, A.H. Strømman, K. Tanaka, A. Levasseur, Bridging the gap between impact assessment methods and climate science, Environ. Sci. Policy. 64 (2016) 129–140. https://doi.org/10.1016/j.envsci.2016.06.019.

[24] O. Jolliet, A. Antón, A.M. Boulay, F. Cherubini, P. Fantke, A. Levasseur, T.E. McKone, O. Michelsen, L. Milà i Canals, M. Motoshita, S. Pfister, F. Verones, B. Vigon, R. Frischknecht, Global guidance on environmental life cycle impact assessment indicators: impacts of climate change, fine particulate matter formation, water consumption and land use, Int. J. Life Cycle Assess. 23 (2018) 2189–2207. https://doi.org/10.1007/s11367-018-1443-y.

[25] J. Giuntoli, S. Caserini, L. Marelli, D. Baxter, A. Agostini, Domestic heating from forest logging residues: Environmental risks and benefits, J. Clean. Prod. 99 (2015) 206–216. https://doi.org/10.1016/j.jclepro.2015.03.025.

[26] A. Levasseur, P. Lesage, M. Margni, R. Samson, Biogenic Carbon and Temporary Storage Addressed with Dynamic Life Cycle Assessment, J. Ind. Ecol. 17 (2013) 117–128. https://doi.org/10.1111/j.1530-9290.2012.00503.x.

[27] G.P. Peters, B. Aamaas, M. T. Lund, C. Solli, J.S. Fuglestvedt, Alternative “global warming”

metrics in life cycle assessment: A case study with existing transportation data, Environ. Sci. Technol. 45 (2011) 8633–8641. https://doi.org/10.1021/es200627s.

[28] T. Hammar, F. Levihn, Time-dependent climate impact of biomass use in a fourth generation district heating system, including BECCS, Biomass and Bioenergy. 138 (2020) 105606. https://doi.org/10.1016/j.biombioe.2020.105606.

[29] R. Green, Optimising bioenergy use in district heating systems in the EU, University of Bath, Bath, UK, 2019. https://researchportal.bath.ac.uk/en/studentTheses/optimising-bioenergy-use-in-district-heating-systems-in-the-eu.

[30] J. Neeft, BioGrace II, Intell. Energy Eur. Program. (2015). https://biograce.net/app/webroot/biograce2/.

[31] M. Röder, E. Thiffault, C. Martínez-Alonso, F. Senez-Gagnon, L. Paradis, P. Thornley, Understanding the timing and variation of greenhouse gas emissions of forest bioenergy systems, Biomass and Bioenergy. 121 (2019) 99–114. https://doi.org/10.1016/j.biombioe.2018.12.019.

[32] IPCC, Anthropogenic and Natural Radiative Forcing, in: Intergovernmental Panel on Climate Change (Ed.), Clim. Chang. 2013 - Phys. Sci. Basis, Cambridge University Press, Cambridge, n.d.: pp. 659–740. https://doi.org/10.1017/CBO9781107415324.018.

[33] O. Boucher, M.S. Reddy, Climate trade-off between black carbon and carbon dioxide emissions, Energy Policy. 36 (2008) 193–200. https://doi.org/10.1016/j.enpol.2007.08.039.

[34] S. Cooper, Temporal Climate Impacts, (2020). https://doi.org/https://doi.org/10.15125/BATH-00923.

[35] A. Agostini, J. Giuntoli, L. Marelli, S. Amaducci, Flaws in the interpretation phase of bioenergy LCA fuel the debate and mislead policymakers, Int. J. Life Cycle Assess. 25 (2020) 17–35. https://doi.org/10.1007/s11367-019-01654-2.

[36] D.T. Shindell, G. Faluvegi, D.M. Koch, G.A. Schmidt, N. Unger, S.E. Bauer, Improved Attribution of Climate Forcing to Emissions, Science (80-.). 326 (2009) 716–718. https://doi.org/10.1126/science.1174760.

Appendix A – Alternative form of equations for spreadsheet

To make the calculations work efficiently in a spreadsheet, the standard presentation of AGWP and AGTP equations was rearranged. This appendix details these changes for convenience to other researchers creating similar tools. Non-CO_2 WMGHGs are considered first before treatment is expanded to include the multi-component decay of CO_2.

The mass of species i (that decays with a simple exponential form) remaining in the atmosphere at [the start of] year-T after a pulse X_0 at [the start of] year-0 is given by:

$$M_i(t) = X_{i,0}e^{-\frac{T}{\tau_i}}$$

Where τ_i is the perturbation lifetime.

For a time-series of pulse emissions of species i, occurring at [the start of] years {0, 1 … t } the mass remaining at [the start of] year-t could be calculated by summing the prevalence due to each pulse:

$$M_i(t) = X_{i,0}e^{-\frac{t}{\tau_i}} + X_{i,1}e^{-\frac{t-1}{\tau_i}} + \cdots + X_{i,t-1}e^{-\frac{1}{\tau_i}} + X_{i,t}$$

If results are only required for a particular year t, then this is an efficient approach (taking O(t) time). However, if we also require a time-series of results (e.g. the mass in each year up to year-T) then it becomes more intensive (taking $O(T^2/2)$). Although a spreadsheet-based tool can provide good transparency, it can rapidly become unusable in this situation.

In this case, a recursive approach is more efficient. Here, for each year, we calculate the remaining mass due as the sum of the emission pulse that year and the mass due to previous years. This approach takes O(T); i.e. for a 500-year horizon, it is almost 250-times more efficient:

$$M_i(t) = M_{i,t-1}\, e^{-\frac{1}{\tau_i}} + X_{i,t}$$

Where $M_{i,t-1} = M_{i,t-2}\, e^{-\frac{1}{\tau_i}} + X_{i,t-1}$ and so on back to $M_{i,0}$.

Note that while we are taking a one-year time-step as convenient and sufficient for our purposes, a different time-step could be applied (for example a shorter time-step to study combined effect of different intra-year emissions). In this case, the numerator of the fraction that e is raised to would need to be adjusted. So more generally:

$$M_i(t) = M_{i,t-timestep}\, e^{-\frac{timestep}{\tau_i}} + X_{i,t}$$

A similar approach can be applied to AGWP:

$$AGWP_i(t) = AGWP_{i,(t-1)} + A_i \tau_i M_{i,t-1}(1 - e^{-\frac{1}{\tau_i}})$$

Where A_i is the specific radiative forcing for species i. Note that convention here is effectively to evaluate $AGWP_t$ and $AGTP_t$ before the pulse emission for that year (X_t) has had time to have any effect but the calculation for M_t does include it.

Because we use a two-component surface temperature response (as per [9,33]), the expression of AGTP is more complicated. Each component of the temperature response (at each time-step) has to be calculated separately based on its value at the last time-step and *then* summed:

$$AGTP_i(t) = AGTP_{1,i,(t-1)}\, e^{-\frac{1}{d_1}} + A_i \tau_i M_{i,t-1} \frac{c_1}{\tau_i - d_1}(e^{-\frac{1}{\tau_i}} - e^{-\frac{1}{d_1}})$$

$$+ AGTP_{2,i,(t-1)}\, e^{-\frac{1}{d_2}} + A_i \tau_i M_{i,t-1} \frac{c_2}{\tau_i - d_2}(e^{-\frac{1}{\tau_i}} - e^{-\frac{1}{d_2}})$$

Where c , and d are the climate sensitivity and response time, and $AGTP_1$, c_1 , and d_1 relate to first component of temperature response while $AGTP_2$, c_2 , and d_2 relate to the second component.

For CO_2, the approach is the same but (similar to the AGTP calculation), each component of its decay needs to be calculated based on the previous time-step for that component, and *then* summed together:

$$M_{CO2}(t) = \left[M_{0,t-1} + X_t a_0\right] + \sum_{j=1}^{3}\left[M_{j,t-1}e^{-\frac{1}{\tau_j}} + X_t a_j\right]$$

Where a_0 to a_3 refer to the proportions of CO_2 with no decay or decay exponents τ_j. Note that the four masses of CO_2 (M_0 to M_3) need to be stored for each time-step as they are used individually to calculate result for next step. Similar forms are available for $AGWP_{CO2}$ and $AGTP_{CO2}$, dependent upon the result for the previous time-step and the different mass components from it:

$$AGWP_{CO2}(t) = AGWP_{CO2,(t-1)} + A_{CO2}\left[M_{0,t-1} + \sum_{j=1}^{3}\tau_j M_{j,t-1}\left(1 - e^{-1/\tau_j}\right)\right]$$

$$AGTP_i(t) = AGTP_{1,i,(t-1)}\, e^{-\frac{1}{d_1}} + A_i\tau_i G_{i,t-1}\frac{c_1}{\tau_i - d_1}\left(e^{-\frac{1}{\tau_i}} - e^{-\frac{1}{d_1}}\right)$$

$$+ AGTP_{2,i,(t-1)}\, e^{-\frac{1}{d_2}} + A_i\tau_i G_{i,t-1}\frac{c_2}{\tau_i - d_2}\left(e^{-\frac{1}{\tau_i}} - e^{-\frac{1}{d_2}}\right)$$

$$AGTP_{CO2}(t) =$$

$$\sum_{k=1}^{2}\left\{AGTP_{k,t-1}\, e^{-\frac{1}{d_k}} + A_{CO2}\left[M_{0,t-1}\, c_k\left(1 - e^{-\frac{1}{d_k}}\right) + \sum_{j=1}^{3}\frac{\tau_j M_{j,t-1}\, c_k}{\tau_j - d_k}\left(e^{-1/\tau_j} - e^{-1/d_k}\right)\right]\right\}$$